New Measurement of the Properties of the Rare Decay $K^+ \to \pi^+ e^+ e^-$

R. Appel,[6,3] G. S. Atoyan,[4] B. Bassalleck,[2] D. R. Bergman,[6,*] D. N. Brown,[3,†] N. Cheung,[3] S. Dhawan,[6] H. Do,[6] J. Egger,[5] S. Eilerts,[2,‡] C. Felder,[3,1] H. Fischer,[2,§] M. Gach,[3,‖] W. Herold,[5] V. V. Issakov,[4] H. Kaspar,[5] D. E. Kraus,[3] D. M. Lazarus,[1] L. Leipuner,[1] P. Lichard,[3] J. Lowe,[2] J. Lozano,[6,¶] H. Ma,[1] W. Majid,[6,**] W. Menzel,[7,††] S. Pislak,[8,6] A. A. Poblaguev,[4] V. E. Postoev,[4] A. L. Proskurjakov,[4] P. Rehak,[1] P. Robmann,[8] A. Sher,[3] T. L. Thomas,[2] J. A. Thompson,[3] P. Truöl,[8,6] H. Weyer,[7,5] and M. E. Zeller[6]

[1]*Brookhaven National Laboratory, Upton Long Island, New York 11973*
[2]*Department of Physics and Astronomy, University of New Mexico, Albuquerque, New Mexico 87131*
[3]*Department of Physics and Astronomy, University of Pittsburgh, Pittsburgh, Pennsylvania 15260*
[4]*Institute for Nuclear Research of Russian Academy of Sciences, Moscow 117312, Russia*
[5]*Paul Scherrer Institut, CH-5232 Villigen, Switzerland*
[6]*Physics Department, Yale University, New Haven, Connecticut 06511*
[7]*Physikalisches Institut, Universität Basel, CH-4046 Basel, Switzerland*
[8]*Physik-Institut, Universität Zürich, CH-8057 Zürich, Switzerland*

(Received 21 July 1999)

A low-background sample of 10 300 events has been collected for the decay mode $K^+ \to \pi^+ e^+ e^-$ by experiment E865 at the Brookhaven Alternating Gradient Synchrotron. The branching ratio is measured to be $[2.94 \pm 0.05(\text{stat}) \pm 0.13(\text{syst}) \pm 0.05(\text{model})] \times 10^{-7}$, the vector nature of this decay is firmly established, and the decay form factor $f(z) = f_0(1 + \delta z)(z = M_{ee}^2/m_K^2)$ is determined to have $\delta = 2.14 \pm 0.13 \pm 0.15$. The experiment is described and results discussed in the context of chiral perturbation theory.

PACS numbers: 13.20.Eb, 11.30.Hv, 12.39.Fe

The decay $K^+ \to \pi^+ e^+ e^-$ ($K_{\pi ee}$) proceeds via a flavor changing neutral current and is highly suppressed by the Glashow-Iliopoulos-Maiani (GIM) mechanism. The decay rate was first calculated [1] assuming a short-distance $s \to d\gamma$ transition at the quark level. Later it was realized that the long-distance effects dominate the decay mechanism [2]. Several recent calculations, which study the rate and invariant electron-positron mass (M_{ee}) distributions, were performed within the framework of chiral QCD perturbation theory (ChPT) [3–5], an approach which has been quite successful at describing many decay modes of the light mesons, e.g., semileptonic and radiative kaon decays [6].

The first few events for this decay were observed at CERN [7]. Two subsequent experiments at the Brookhaven Alternating Gradient Synchrotron (AGS), E777 [8] and E851 [9], observed 500 and 800 events, and measured branching ratios of 2.75 ± 0.26 and 2.81 ± 0.20 ($\times 10^{-7}$), respectively. We report here the results of a new measurement with larger acceptance and significantly increased statistics. Our data allow a detailed study of the decay form factor and a comparison with ChPT calculations and other models.

The experiment was performed at the Brookhaven National Laboratory's AGS. The apparatus, a schematic drawing of which is shown in Fig. 1, was constructed to search for the decay $K^+ \to \pi^+ \mu^+ e^-$ [10–13]. It resided in a 6 GeV/c unseparated beam containing about 10^8 K^+ and 2×10^9 π^+ and protons per 1.6 s AGS pulse.

Downstream of a 5-m-long evacuated decay volume a dipole magnet separated the trajectories by charge, with negative particles going mainly to the left. This was followed by a spectrometer consisting of four proportional chambers surrounding a dipole magnet with a 0.833 T m field integral, which determined the momenta and trajectories of the decay products. Particle identification was accomplished with Čerenkov counters filled with H_2 on the left (C1L and C2L), and CH_4 on the right (C1R and C2R) at atmospheric pressure; with an electromagnetic

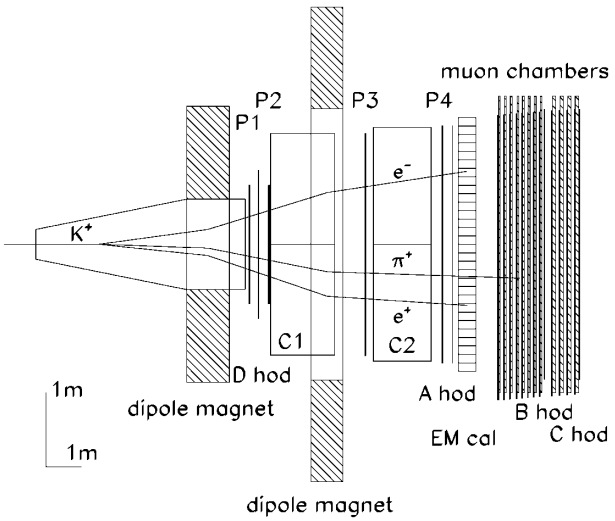

FIG. 1. Plan view of the E865 detector. P1–P4: proportional chambers; C1, C2: Čerenkov counters; A,B,C,D: scintillator hodoscopes. The beam passes through holes in the calorimeter and muon stack, dead regions in the proportional chambers, He bags and H_2 filled beam tubes in the Čerenkov counters, which are not shown here.

 0031-9007/99/83(22)/4482(4)$15.00

calorimeter of the Shashlik design [14], consisting of 600 modules, each 11.4 cm by 11.4 cm by 15 radiation lengths in depth, arrayed 30 horizontally and 20 vertically; and with a muon range stack consisting of 24 planes of proportional tubes situated between iron plates. With these components, electrons were identified as having light in the appropriate Čerenkov counters and energy in the calorimeter consistent with the measured momentum of the trajectory. Pions were identified as having no light in the Čerenkov counters, and an energy loss in the calorimeter consistent with that of a minimum ionizing particle or a hadron shower. Compared to the most recent experiment [8,9] the E865 spectrometer had improved particle identification capabilities, spectrometer resolution, and larger, more uniform acceptance.

The first-level trigger for the experiment is based on three charged particle hits using hodoscopes D and A (arrays of 10 and 15 slats each on either side of the beam line, respectively), and the calorimeter. Most of the rate at this stage comes from accidentals, and $K^+ \to \pi^+\pi^+\pi^-$ (K_τ) decays. For $K_{\pi ee}$ decays the next level trigger required Čerenkov counter signals on each side of the detector. This trigger was dominated by events from the decay chain $K^+ \to \pi^+\pi^0$; $\pi^0 \to e^+e^-\gamma$ (K_{dal}) with low invariant mass M_{ee}. To enhance the fraction a high mass trigger was configured, in which events with small vertical separation of calorimeter hits were prescaled. This reduced the number of K_{dal} triggers, while keeping 85% of the high M_{ee} events. Figure 2 shows the invariant mass spectra for the prescaled monitor K_{dal} events and those which were accepted by this trigger and were used for normalization.

In the analysis, the basis for the selection of both normalization and signal events was the unambiguous identification of a positive pion and lepton pair with trajectories from a common vertex located within the decay volume. With a cut $M_{ee} > 0.15$ GeV we have a nearly pure sample of $K_{\pi ee}$ events with a three particle invariant mass $M_{\pi ee} \approx m_K$, as shown in Fig. 3. The onset of the K_{dal} events can be seen for $M_{ee} < 0.13$ GeV and $M_{\pi ee} < m_K$, the latter because of a missing photon. For $K_{\pi ee}$ events, the reconstructed K^+ was required to come from the production target within the limits inferred from studying K_τ decays. Our final signal sample contains 10 300 $K_{\pi ee}$ candidates including 1.2% background events. Our normalization sample, after prescaling, contains 10^5 K_{dal} candidates including a 17% contribution from two other K^+ decays giving π^0-Dalitz pairs ($K^+ \to \pi^0\mu^+\nu_\mu$ with the μ^+ treated as a π^+, and $K^+ \to \pi^+\pi^0\pi^0$). The inset in Fig. 3 exhibits a $M_{\pi ee}$ mass resolution of $\sigma = 5.7$ MeV, in good agreement with the Monte Carlo simulation. The calculated M_{ee} resolution is $\sigma = 4.8$ MeV nearly independent of M_{ee}.

The acceptance for $K_{\pi ee}$ and K_{dal} events was determined to be 0.73% and 0.85%, respectively, with a Monte Carlo simulation, which included the geometry of beam line and spectrometer, and the separately measured efficiencies and responses of scintillators, proportional chambers, Čerenkov and shower counters. The acceptance varies smoothly within ±15% over the mass range $0.15 < M_{ee} < 0.35$ GeV. The influence of the efficiencies on the acceptance nearly cancels in the normalization, since $K_{\pi ee}$ and K_{dal} events contain the same final states, and their different spatial distributions produce only minor differences, and are taken into account. For K_{dal} events the matrix elements of [15] were used for $\pi^0 \to e^+e^-\gamma$, and the theoretical input to the $K_{\pi ee}$ simulation is discussed below. Figure 2 demonstrates that the major difference between $K_{\pi ee}$ and K_{dal} events, the high-mass

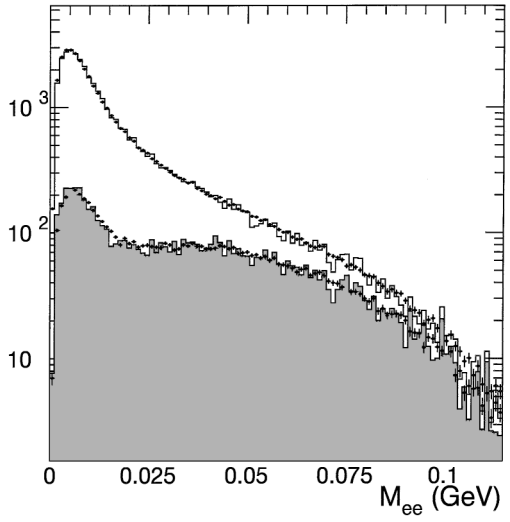

FIG. 2. M_{ee} distribution for accepted K_{dal} events with (lower curve) and without (upper curve) high-mass trigger required. The Monte Carlo simulation (histogram) includes events from other K^+ decays with a π^0 in the final state.

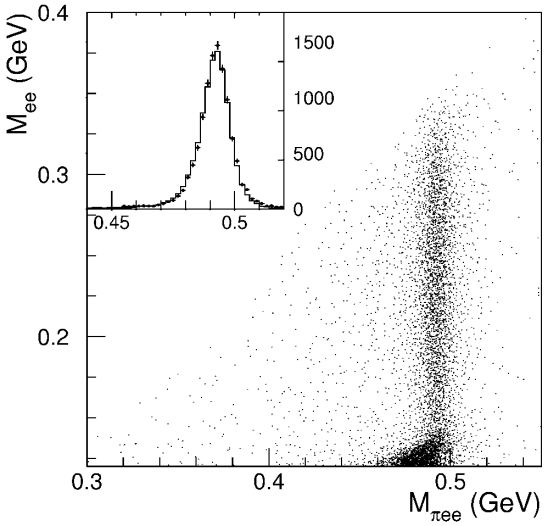

FIG. 3. Scatter plot M_{ee} versus $M_{\pi ee}$ for $K_{\pi ee}$ candidates. Inset: $M_{\pi ee}$ mass for candidates with $M_{ee} > 0.15$ GeV. The histogram shows the Monte Carlo simulation.

trigger, is correctly accounted for, in magnitude as well as in shape. A subsample of 500 $K_{\pi ee}$ events bypassing the high-mass trigger provided an independent check of the trigger acceptance.

The essential distributions necessary for the interpretation of our data are shown in Fig. 4. Since the decay is supposed to proceed through one photon exchange, i.e., by a vector interaction (V) with a decay amplitude [5]

$$\frac{\alpha G_F}{4\pi} f_V(z) P^\mu \overline{u}_e \gamma_\mu u_e ,$$

one expects an angular distribution proportional to $\sin^2\theta$, where θ is the angle between the positron and pion momentum vectors in the center of mass of the e^+e^- pair. The presence of other decay mechanisms, however, may produce small admixtures of scalar (S) or tensor (T) terms [16]. The corresponding decay amplitudes

$$G_F m_K f_S \overline{u}_e u_e \quad \text{or} \quad G_F f_T \frac{P^\mu q^\nu}{m_K} \overline{u}_e \sigma_{\mu\nu} u_e ,$$

lead to either a constant (S) angular distribution or one proportional to $\cos^2\theta$ (T). Here G_F is the Fermi constant, $P = p_K + p_\pi$, $q = p_K - p_\pi$, and the form factors $f_{V,S,T}$ are dimensionless functions of $z = M_{ee}^2/m_K^2$ [17]. Fitting a two-dimensional distribution whose projections are shown in Fig. 4, we find good agreement with a vector interaction. At a 90% confidence level, at most 2% of the branching ratio could result from either scalar or tensor interaction corresponding to constraints $|f_S| < 6.6 \times 10^{-5}$ and $|f_T| < 3.7 \times 10^{-4}$.

Neglecting terms proportional to m_e^2/M_{ee}^2 the mass distribution for a vector interaction can be described by

$$\frac{d\Gamma}{dz} = \frac{G_F^2 \alpha^2 m_K^5}{3(4\pi)^5} \eta^{3/2}(1, z, m_\pi^2/m_K^2) |f_V(z)|^2, \quad (1)$$

where $\eta(a,b,c) = a^2 + b^2 + c^2 - 2ab - 2ac - 2bc$. The form factor $f_V(z)$ can be determined by fitting the observed spectrum in the experimentally accessible range $0.1 < z < 0.51$. We have used two different parametrizations of the form factor, one model independent [Eq. (2)] and the other derived from ChPT [5] [Eq. (3)]:

$$f_V(z) = f_0(1 + \delta z + \delta' z^2), \quad (2)$$

$$f_V(z) = a_+ + b_+ z + w^{\pi\pi}(z). \quad (3)$$

$f_0, \delta, \delta', a_+, b_+$ are free parameters [18], and $w^{\pi\pi}$ is the contribution from a pion loop graph given in [5].

Figure 5 displays the form factor, which is extracted from the ratio of mass distributions for the measured events to events simulated with a constant form factor. The results of our fit to the linear and ChPT ansatz are superimposed. Figure 4 shows the spectrum itself. The parameters and branching ratios are given in Table I. The different contributions to the systematic uncertainty of our results are listed in Table II. Radiative corrections have been included in the simulation following [19]. This increased the branching ratio by 5.5% and the linear slope by 4%.

The inclusion of the quadratic term in the model independent ansatz improves the quality of the fit. The values of δ and δ' are, however, strongly correlated. Our result $\delta = 2.14 \pm 0.13 \pm 0.15$ is in fair agreement with the less precise results of experiment E777 [8,18] $\delta = 1.31 \pm 0.44$. The large value of δ is in contradiction with the meson dominance class of models [20,21], in which the form factor slope is given in first approximation as $\delta = (m_K/m_\rho)^2$.

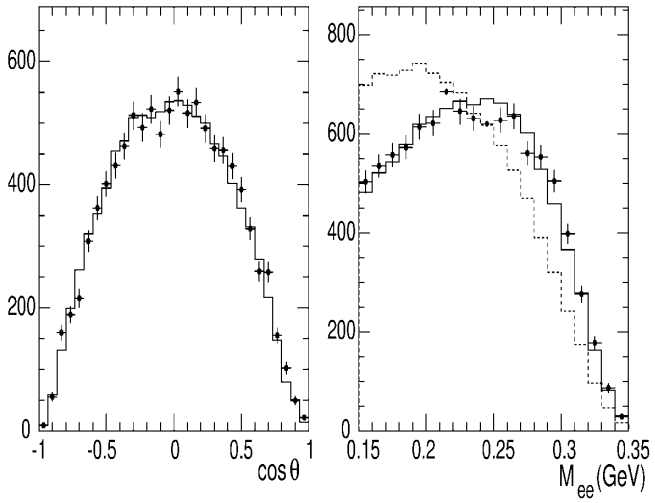

FIG. 4. Angular (left) and invariant mass (right) distributions for events (data points) compared to Monte Carlo simulations (histogram) assuming a pure vector interaction. For illustration the linear form factor parametrization with $\delta = 2.14$ is used. The dashed histogram (right) corresponds to a constant form factor ($\delta = 0$).

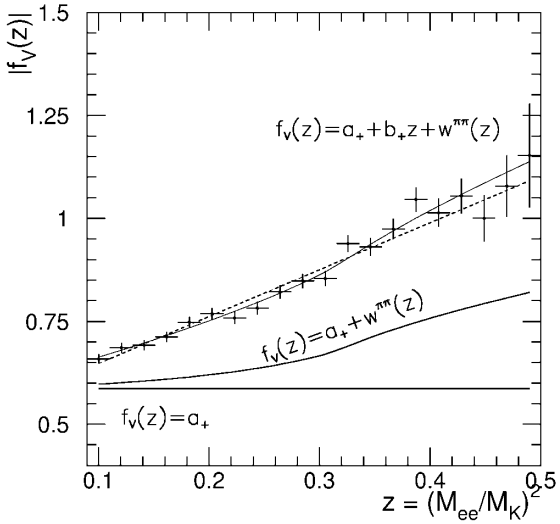

FIG. 5. The measured form factor $|f_V(z)|$ versus z. The dashed line shows the linear fit [Eq. (2) with $\delta' = 0$]. The labeled solid lines refer to the next-to-leading-order ChPT fit [Eq. (3)]. The constant and pion loop graph contributions are explicitly displayed.

TABLE I. Summary of results for the fits to the measured form factor. The branching ratios (B) are given in units of (10^{-7}). B (meas) corresponds to $M_{ee} > 0.15$ GeV and is within the statistical error independent of the parametrization of the form factor.

	Eq. (2)		Eq. (3)
f_0	0.533 ± 0.012	0.591 ± 0.027 a_+	-0.587 ± 0.010
δ	2.14 ± 0.13	0.97 ± 0.44 b_+	-0.655 ± 0.044
δ'	0	1.99 ± 0.67	...
$\chi^2/n_{\text{d.o.f.}}$	22.9/18	16.6/17	13.3/18
B (total)	2.884 ± 0.037	2.991 ± 0.058	2.988 ± 0.040
B (meas)		2.015 ± 0.020	

The ChPT parametrization of Eq. (3) includes the contribution from the pion loop graph. This term has a strong z dependence, which has not been calculated explicitly in most earlier models. In the first, lowest nontrivial order ChPT calculation [$\mathcal{O}(p^4)$] [3] the pion loop graph was assumed to be the only significant source of z dependence of the form factor (i.e., $b_+ = 0$). Our data show that this is a poor approximation. Significant z dependence from other terms is expected in next-to-leading-order ChPT [4,5]. The amplitude linear in z [Eq. (3)], which ChPT cannot calculate, represents all contributions other than the pion loop term [5]. The substantial reduction in the value of χ^2 which is observed when the pion loop term is included provides direct experimental evidence for its small but important contribution to describing the curvature of the form factor.

Summarizing the results of our analysis we conclude: (i) the experimental data are consistent with a vector model for the interaction, (ii) the slope of the form factor is significantly larger than meson dominance or leading order ChPT models predict, and (iii) although a linear approximation of the form factor is reasonable, our data indicate a nonlinearity of the form factor which is fit well by the ChPT loop term. Our final result for the total branching ratio is $[2.94 \pm 0.05(\text{stat}) \pm 0.13(\text{syst}) \pm 0.05(\text{model})] \times 10^{-7}$. Here we include the model dependence of the extrapolation into the low-mass region not covered by our detector by taking the average of the extreme values in Table I.

We gratefully acknowledge the contributions to the success of this experiment by Dave Phillips, the staff and management of the AGS at the Brookhaven National Laboratory, and the technical staffs of the participating institutions. This work was supported in part by the U.S. Department of Energy, the National Science Foundations of the U.S., Russia, and Switzerland, and the Research Corporation.

TABLE II. Summary of systematic errors. The reconstruction and background subtraction error result from adding several smaller contributions linearly. The total error is the sum of the four groups in quadrature.

Source	σ_B/B (%)	σ_δ/δ (%)
Normalization to $\pi^0 \to e^+e^-\gamma$	2.8	...
Radiative corrections	1.4	0.5
Reconstruction (including trigger)	3.0	6.5
Background subtraction	1.5	2.3
Total	4.5	6.9

*Present address: Rutgers University, Piscataway, NJ 08855.
†Present address: University of Louisville, Louisville, KY 40292.
‡Present address: University of Texas, Austin, TX 78712.
§Present address: Albert-Ludwigs-Universität, D-79104 Freiburg, Germany.
‖Present address: GE Medical Systems, Milwaukee, WI 53201.
¶Present address: University of Connecticut, Storrs, CT 06269.
**Present address: LIGO/Caltech, Pasadena, CA 91125.
††Present address: Universitätspital, CH-8091 Zürich, Switzerland.

[1] M. K. Gaillard and B. W. Lee, Phys. Rev. D **10**, 897 (1974).
[2] See [8] for a list of older references.
[3] G. Ecker, A. Pich, and E. de Rafael, Nucl. Phys. **B291**, 692 (1987).
[4] J. Donoghue and F. Gabbiani, Phys. Rev. D **51**, 2187 (1995).
[5] G. D'Ambrosio *et al.*, JHEP **8**, 4 (1998).
[6] See, e.g., G. D'Ambrosio *et al.*, in *Second DAPHNE Physics Handbook*, edited by L. Maiani *et al.* (Laboratori Nazionali de Frascati, Frascati, Italy, 1995), p. 265; J. Bijnens, G. Ecker, and J. Gasser, *ibid.*, p. 125; J. Bijnens, in Proceedings of the Chicago Conference on Kaon Physics, Chicago, 1999 (hep-ph/9907514, 1999).
[7] P. Bloch *et al.*, Phys. Lett. B **56**, 201 (1975).
[8] C. Alliegro *et al.*, Phys. Rev. Lett. **68**, 278 (1992).
[9] A. L. Deshpande, Ph.D. thesis, Yale University, 1995.
[10] R. Appel *et al.*, Nucl. Instrum. Methods (to be published).
[11] S. Pislak, Ph.D. thesis, University of Zürich, 1997.
[12] D. R. Bergman, Ph.D. thesis, Yale University, 1997.
[13] S. Eilerts, Ph.D. thesis, University of New Mexico, 1998.
[14] G. S. Atoyan *et al.*, Nucl. Instrum. Methods Phys. Res., Sect. A **320**, 144 (1992).
[15] K. O. Mikaelian and J. Smith, Phys. Rev. D **5**, 1763 (1973).
[16] S. W. MacDowell, Ann. Phys. (N.Y.) **18**, 171 (1962); D. S. Beder, and G. V. Dass, Phys. Lett. B **59**, 444 (1975).
[17] Any relevant coupling constants which might appear in the Lagrangian have been absorbed in the definitions of f_S and f_T.
[18] The parameter δ used here relates to the parameter λ used in [8] as $\delta = \lambda(m_K/m_\pi)^2$.
[19] B. E. Lautrup and J. Smith, Phys. Rev. D **3**, 1122 (1971).
[20] P. Lichard, Phys. Rev. D **55**, 5385 (1997); **60**, 053007 (1999); University of Pittsburgh, Report No. hep-ph/9904265.
[21] L. Bergström and P. Singer, Phys. Rev. D **43**, 1568 (1991); Phys. Rev. Lett. **55**, 2633 (1985).